NUMERICAL SIMULATION AND EXPERIMENTAL FLUTTER RESEARCH OF AN AIRCRAFT WITH ASYMMETRIC CONTROL SURFACES

O.A. Orlova[1], M.A. Pronin[1], V.I. Smyslov [1]

[1] Aeroelasticity Department, TsAGI
1, Zhukovsky str., Zhukovsky, Moscow Region, Russia, 140180
olga.ai.orlova@gmail.com
pronin_m@pochta.ru
smysl@mail.ru

Keywords: aeroelasticity, flutter, asymmetry, numerical simulation, electromechanical modeling.

Abstract: Flutter research of the elastic model of a maneuverable aircraft. Asymmetry of the construction is caused by design features which lead to asymmetry of eigen modes with respect to vertical plane. The results of calculations and experiment are compared.

1 INTRODUCTION

Flutter research of any aircraft includes both parametrical calculations and various ground tests. Numerical calculations for all flight conditions of aircraft and experiment that takes into account all the features of full-scale design complement each other.

The aim of this work was to conduct flutter calculations using different mathematical models with different design schematizations and aerodynamic theories and comparison with experimental results from ground vibration tests (GVT) [1] and from electromechanical modeling (EMM) of aerodynamic forces [2].

In practice, in computational parametric flutter research it's appropriate to use mathematical elastic-mass model symmetrical with respect to geometrical plane of symmetry.

The main distinctive feature of considered aircraft design was difference in stiffness of controls surfaces which was caused by stiffness variation of corresponding actuators. This stiffness difference leads to "splitting" of eigen frequencies and asymmetry of eigen mode shapes, and as a result, specific behavior of the aircraft during flutter.

2 WORK DESCRIPTION

This paper presents flutter research of elastic model of a free aircraft. The geometrical model of the aircraft under study is symmetrical with respect to vertical plane while elastic-mass model is asymmetrical due to stiffness difference between right and left horizontal all-moving control surfaces.

Initial dynamic elastic-mass mathematical models were modified by the results of GVT. First eigen mode was the body vertical bending. Next four eigen modes showed asymmetric behavior. Conventional names of these modes were: symmetric vertical bending of control surfaces with different amplitudes between both surfaces, antisymmetric rotation of the left

control surface and vertical bending of the right control surface, antisymmetric vertical bending of the right control surface and rotation of the left control surface, symmetric rotation of control surfaces with different rotation angles of both surfaces.

There were three mathematical models: one is a beam-based model with quasisteady aerodynamics (TsAGI software package "RIF"), second is a beam-shell model with linearized unsteady aerodynamics similar to doublet lattice method (DLM) (TsAGI software package "KC-M" [3]) and a third one is a finite element method model containing point, beam and shell elements with DLM aerodynamics (MSC.Nastran [4]). Aerodynamic theory used in the experiment with EMM is also linearized unsteady theory with several differences from aerodynamic theory used in KC-M.

Since determinative flutter mode shapes were associated with control surfaces, the bulk of the work was carried out with their vibrations. Obtaining numerical eigen modes spectrum close to experimental of aircraft without air flow refers to a class of "inverse problems" that do not have a unique solution. The process of correction of elastic-mass mathematical models was a labor intensive process including verification of stiffness parameters of rigid support of the control surfaces.

2.1 Eigen modes

The distribution of eigen modes is further represented by two configurations of model for each program, since small changes in the distribution of frequencies could significantly change flutter characteristics. Configurations differed in different values of the stiffnesses of the control surfaces.

In Table 1 the values of the experimental and calculated eigen frequencies for Configuration 1 are shown. Relative difference between numerical eigen frequencies and experimental is marked with "%".

Mode	Description	KC-M		Nastran		RIF		GVT
		f, Hz	*%*	*f*, Hz	*%*	*f*, Hz	*%*	*f*, Hz
1	Body vertical bending	9.80	2.0	9.95	0.5	9.89	1.1	10.00
2	Symmetric bending of control surfaces	14.40	-0.7	14.26	0.2	14.58	-2.0	14.30
3	Antisymmetric rotation of left control surface and vertical bending of right control surface	---	---	---	---	---	---	16.25
4	Antisymmetric vertical bending of right control surface and rotation of left control surface	16.34	5.7	16.19	6.6	16.45	5.1	17.33
5	Symmetric rotation of control surfaces	20.44	-1.6	20.52	-2.0	20.03	0.4	20.12

Table 1: Experimental and numerical eigen modes comparison. Configuration 1.

In the experiment the design of the model of the aircraft contained an elastically suspended actuator, but in mathematical schemes it was rigidly fixed. There are two close eigen modes in GVT – mode 3 (84 Hz) and mode 4 (90 Hz), but in all mathematical models was only one of them. These modes are characterized by antisymmetric motion of control surfaces: while the left control surface is rotating the right control surfaces if bending. In mode 3 the resonance was determined by the left control surface, in mode 4 by the right control surface.

In Configuration 1 mode 2 has a frequency about 74 Hz. Mode 3 in calculations is absent, mode 4 has a frequency close to 84 Hz. Mode 5 has a frequency about 105 Hz. This order of eigen modes strongly influenced critical speed, frequency of flutter and its shape. As can be seen in Table 1 the difference from the experiment didn't exceed 7%.

In Table 2 the values of the experimental and calculated eigen frequencies for Configuration 2 are shown. Relative difference between numerical eigen frequencies and experimental is marked with "%".

Mode	Description	KC-M		Nastran		RIF		GVT
		f, Hz	*%*	*f*, Hz	*%*	*f*, Hz	*%*	*f*, Hz
1	Body vertical bending	9.82	1.8	9.95	0.5	9.89	1.1	10.00
2	Symmetric bending of control surfaces	13.77	3.7	13.58	5.0	13.71	4.1	14.30
3	Antisymmetric rotation of left control surface and vertical bending of right control surface	16.60	-2.2	16.74	-3.0	16.49	-1.5	16.25
4	Antisymmetric vertical bending of right control surface and rotation of left control surface	---	---	---	---	---	---	17.33
5	Symmetric rotation of control surfaces	19.55	2.9	19.46	3.3	19.50	3.1	20.12

Table 2: Experimental and numerical eigen modes comparison. Configuration 2.

In Configuration 2 mode 2 has a frequency about 70 Hz. Mode 3 has a frequency close to 86 Hz, mode 4 is absent. Mode 5 has a frequency about 100 Hz. As can be seen from Table 1 the difference from the experiment didn't exceed 5%.

Comparison of frequencies for Configuration 1 is also illustrated in Fig. 1 by the plot of the dependence of the calculated frequencies on the experimental values. And for Configuration 2 in Fig. 2.

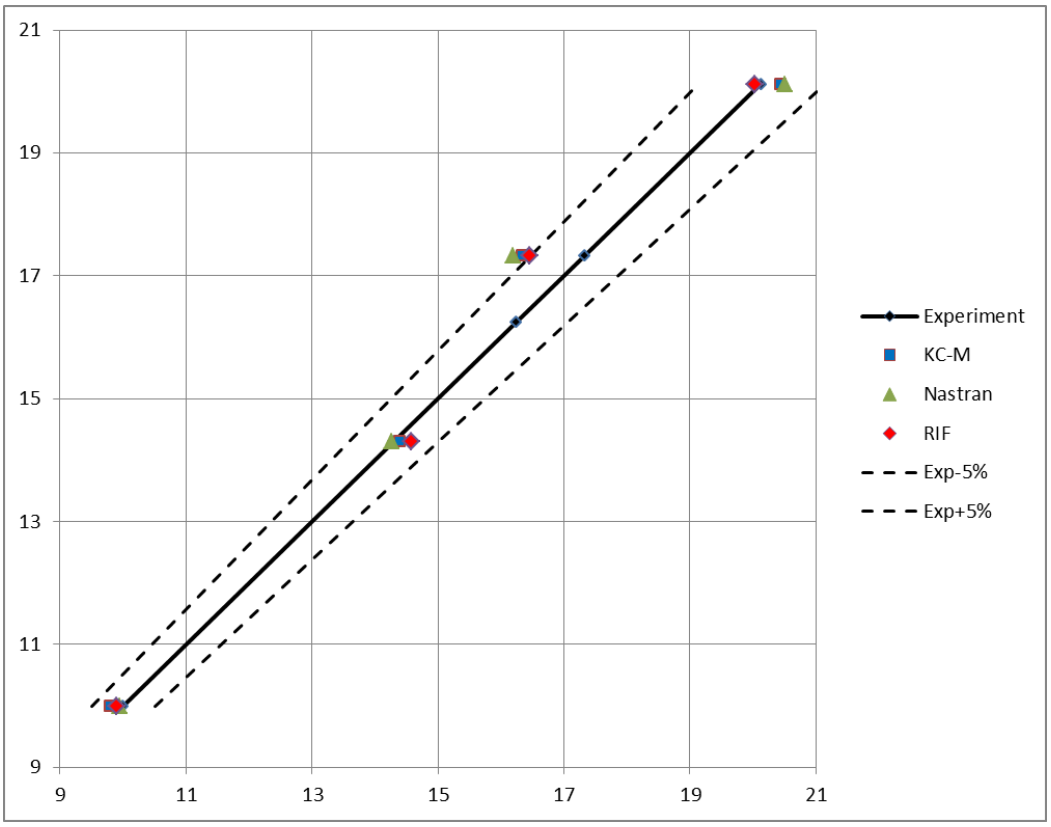

Figure 1: The dependence of the calculated frequencies on the experimental frequencies. Configuration 1.

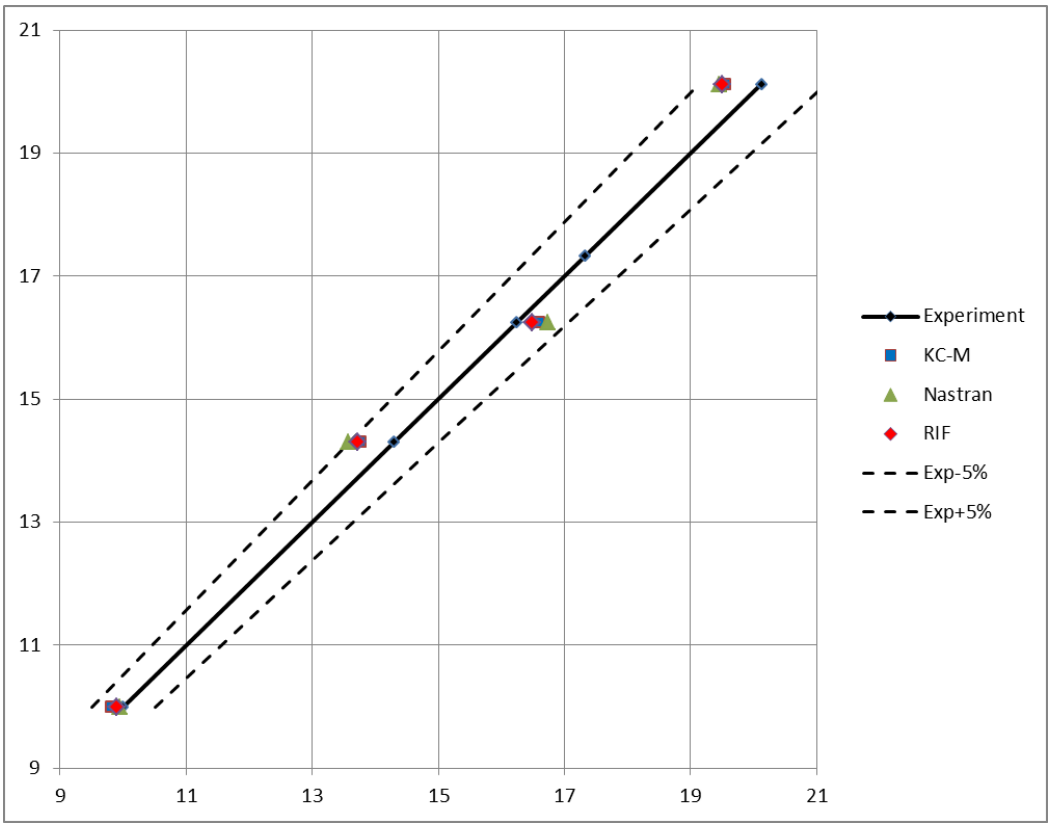

Figure 2: The dependence of the calculated frequencies on the experimental frequencies. Configuration 2.

As can be seen in Fig. 1 and 2 Configuration 2 has the best frequency match.

Mode shapes traditionally have been compared by their titles often rather conditional for higher modes and by the number of nodes or nodal lines that not always explicit. This is qualitative comparison which is not always adequate.

The quantitative comparison concerns numerical position of the nodes for linear unit of aircraft, for example, the beam unit or the angles of slope of the nodal lines for the aggregate surfaces.

In this paper a quantitative comparison of the mode shapes outside the airflow as the values of dimensionless ratios of amplitudes of the characteristic points on control surfaces for different modes is presented.

In Table 3 and 4 amplitudes ratios and rotation angles of left and right control surfaces for experimental and calculated eigen modes for Configuration 1 are given.

Δ_1 – is the ratio of the vibration amplitudes at the point on tip chord on trailing edge to the vibration amplitudes at the point on root cord on trailing edge. Δ_1 – is the same ratio for two points on tip chord and root chord but on leading edge. Ω is the relative rotation angle of control surface which is determined by the ratio of vibration amplitudes at the points on the leading and trailing edges of the root chord on the control surface.

Mode	GVT			КС-М			Nastran			RIF		
	Δ_1	Δ_2	Ω	Δ_1	Δ_2	Ω	Δ_1	Δ_2	Ω	Δ_1	Δ_2	Ω
2	2.32	-0.45	-0.77	2.68	-0.62	-0.74	2.51	-0.57	-0.76	2.50	-0.55	-0.76
3	1.15	0.47	0.88	---	---	---	---	---	---	---	---	---
4	1.12	0.52	0.57	0.88	0.29	0.64	1.05	0.51	0.58	1.00	0.50	0.54
5	-0.84	1.48	0.88	0.42	1.66	0.90	0.58	1.79	0.95	0.43	1.72	0.97

Table 3: Amplitudes ratio and rotation angle for the left control surface. Configuration 1.

Mode	GVT			КС-М			Nastran			RIF		
	Δ_1	Δ_2	Ω	Δ_1	Δ_2	Ω	Δ_1	Δ_2	Ω	Δ_1	Δ_2	Ω
2	7.81	-2.38	-0.15	12.47	-3.31	-0.07	8.85	-3.02	-0.12	9.31	-2.00	-0.10
3	2.68	-1.10	0.58	---	---	---	---	---	---	---	---	---
4	2.41	-0.34	-0.73	2.58	-0.45	-0.79	2.67	-0.48	-0.75	2.63	-0.45	-0.73
5	0.63	0.98	0.90	0.78	1.10	0.79	0.85	0.95	0.88	0.80	0.99	0.92

Table 4: Amplitudes ratio and rotation angle for the right control surface. Configuration 1.

In Table 5 and 6 amplitudes ratio and rotation angles of left and right control surfaces for experimental and calculated eigen modes for Configuration 2 are given.

Mode	GVT			КС-М			Nastran			RIF		
	Δ_1	Δ_2	Ω	Δ_1	Δ_2	Ω	Δ_1	Δ_2	Ω	Δ_1	Δ_2	Ω
2	2.32	-0.45	-0.77	2.45	-0.58	-0.74	2.38	-0.47	-0.80	2.41	-0.51	-0.76
3	1.15	0.47	0.88	1.20	0.38	0.88	1.13	0.52	0.87	1.09	0.56	0.86
4	1.12	0.52	0.57	---	---	---	---	---	---	---	---	---
5	-0.84	1.48	0.88	0.25	1.64	0.80	-0.76	1.50	0.90	-0.79	1.61	0.92

Table 5: Amplitudes ratio and rotation angle for the left control surface. Configuration 2.

Mode	GVT			KC-M			Nastran			RIF		
	Δ_1	Δ_2	Ω	Δ_1	Δ_2	Ω	Δ_1	Δ_2	Ω	Δ_1	Δ_2	Ω
2	7.81	-2.38	-0.15	9.55	-2.98	-0.10	8.01	-2.56	-0.12	8.23	-2.42	-0.12
3	2.68	-1.10	0.58	2.75	-1.21	0.36	2.72	-1.18	0.55	2.71	-1.15	0.56
4	2.41	-0.34	-0.73	---	---	---	---	---	---	---	---	---
5	0.63	0.98	0.90	0.67	1.02	0.87	0.68	0.86	0.90	0.65	0.89	0.92

Table 6: Amplitudes ratio and rotation angle for the right control surface. Configuration 2.

For example mode shapes for Configuration 1 for three mathematical models and experimental one are shown in Fig. 3, for Configuration 2 in Fig. 4. TE is the trailing edge of control surface and LE is the leading edge.

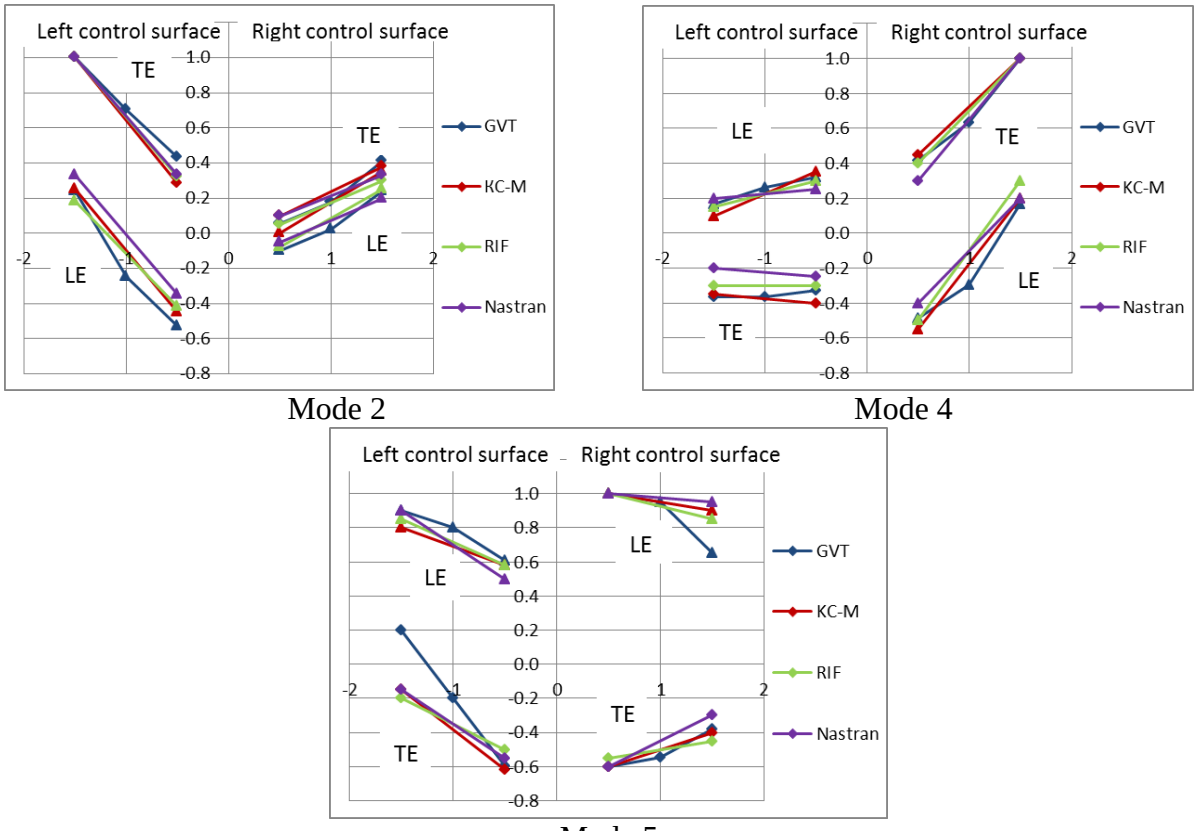

Figure 3: Mode shapes number 2, 4 and 5 for Configuration 1.

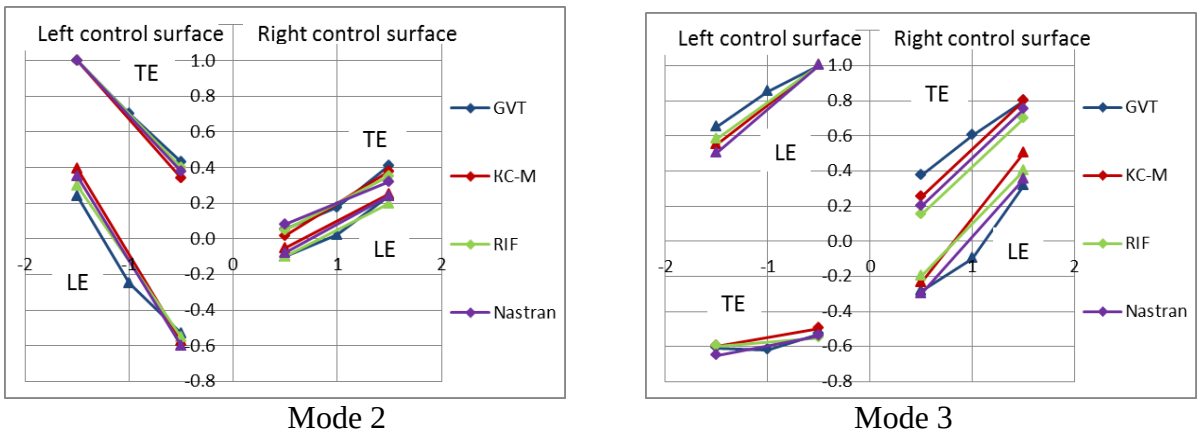

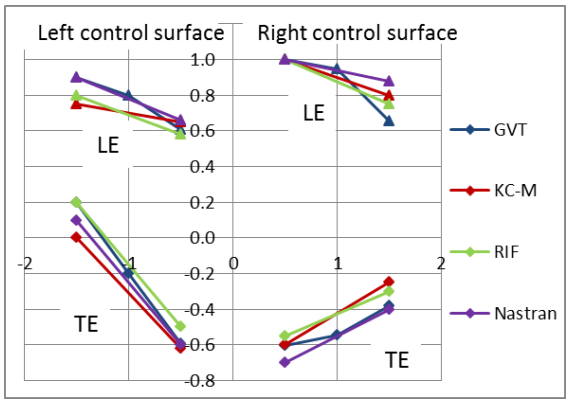

Mode 5

Figure 4: Mode shapes number 2, 3 and 5 for Configuration 2.

As shown in Fig. 3 and 4 relative amplitudes and rotation angles for GVT mode shapes and mathematical models mode shapes are close.

2.2 Flutter characteristic

The results of flutter calculations are presented below as graphs of structural damping against airflow velocity (designation V-g) and current frequency value against airflow velocity (designation V-f.) for Mach = 0.5 and density $\rho = 1.225$ kg/m^3.

In Fig. 5 V-g and V-f graphs for mathematical models for Configuration 1 are shown. On graphs modes number 1, 2, 4 and 5 marked with “1”, “2”, “4” and “5”.

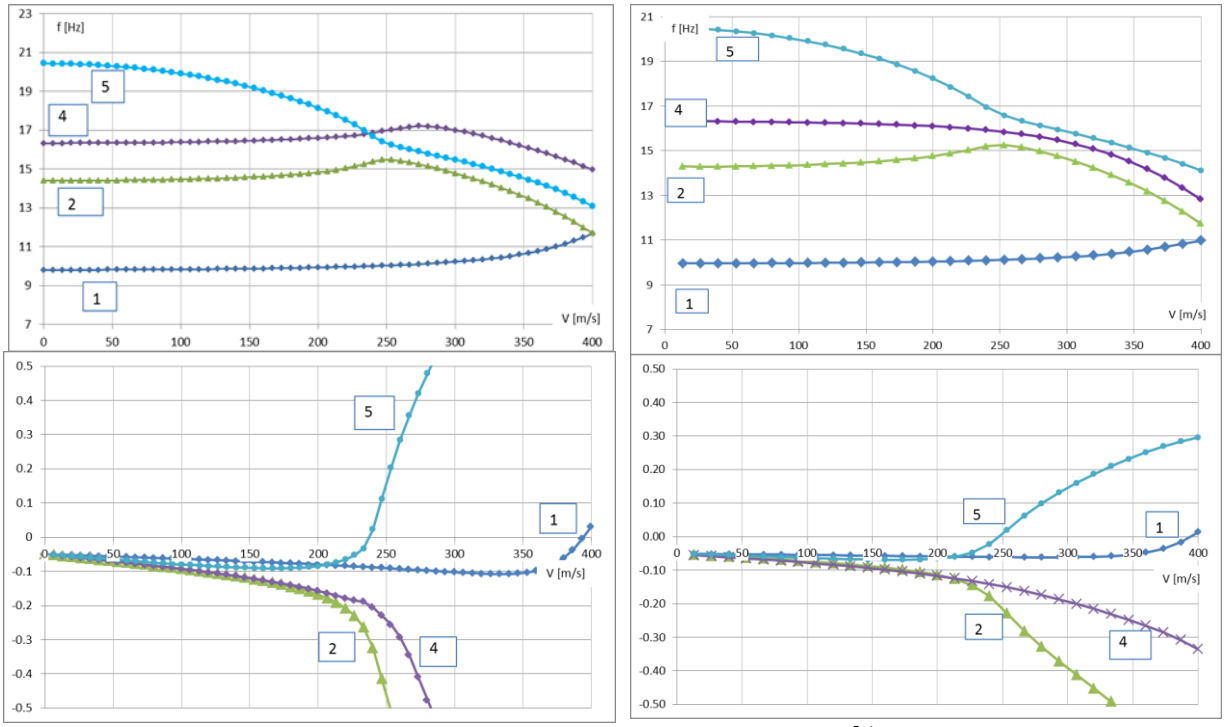

a) KC-M b) Nastran

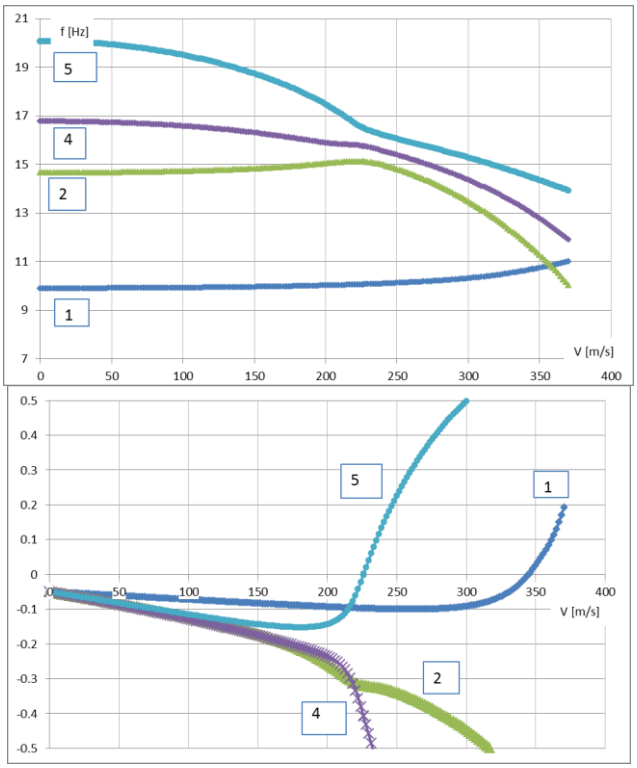

c) RIF

Figure 5: V-f and V-g graphs for: a) KC-M, b) Nastran, c) RIF

As can be seen from the V-f graphs of Configuration 1, there is convergence of modes which determine symmetrical bending of control surfaces (mode 2) and symmetrical rotation of control surfaces (mode 5). On the V-g graph mode 5 (symmetrical rotation of control surfaces) loses stability (curve passes through g = 0). The shape of the flutter mode is characterized by in-phase bending-rotation vibration of right and left control surfaces. Vibrations of the left control surface have greater amplitudes than the right ones.

In Fig. 6 V-g and V-f graphs for mathematical models for Configuration 2 are shown. On graphs modes number 1, 2, 3 and 5 marked with “1”, “2”, “3” and “5”.

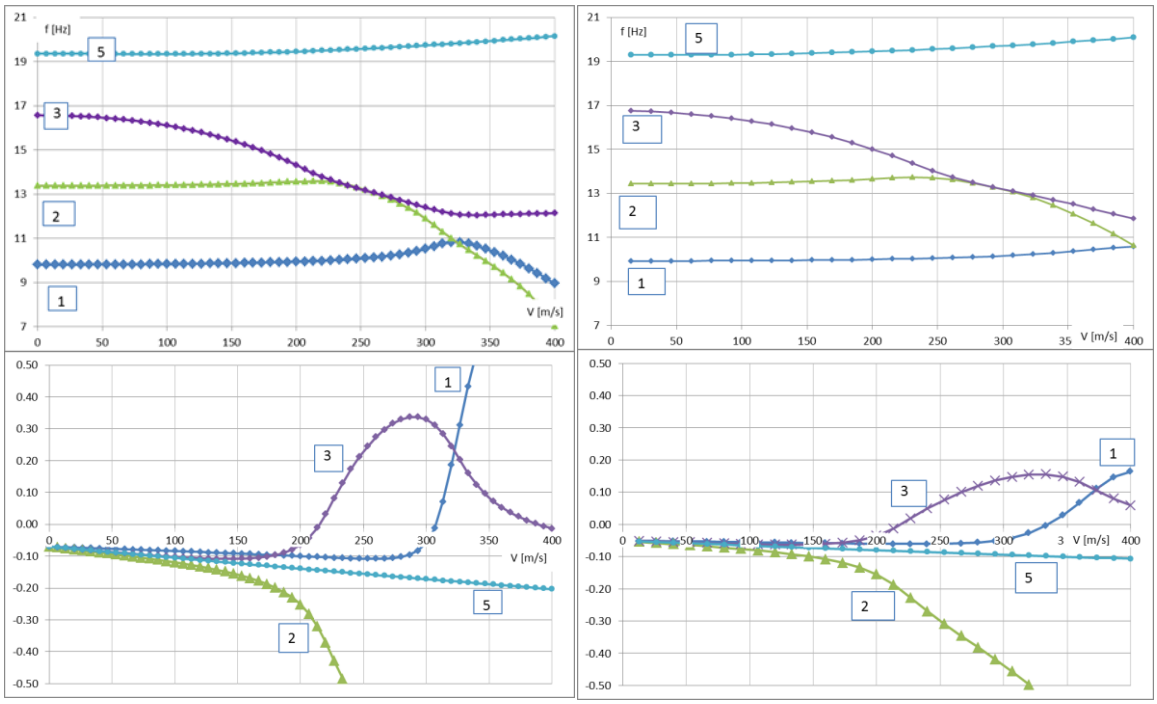

a) KC-M b) Nastran

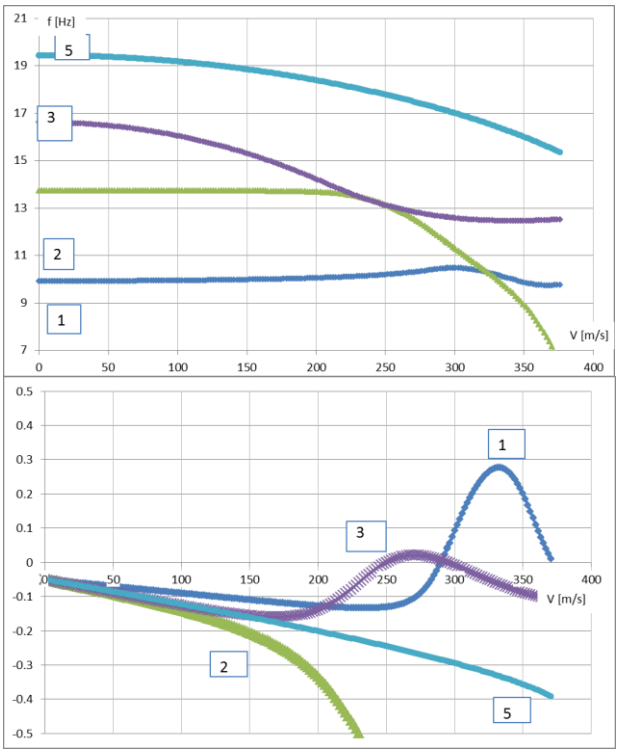

c) RIF

Figure 5: V-f and V-g graphs for: a) KC-M, b) Nastran, c) RIF

As can be seen from the V-f graphs of Configuration 2, there is a convergence of modes which determine symmetrical bending of control surfaces (mode 2) and antisymmetric rotation of left control surfaces and bending of right control surface (mode 3). On the V-g graph mode 3 (antisymmetric rotation of left control surfaces and bending of right control surface) loses stability. After the loss of stability the value of damping becomes positive $g > 0$, with increasing air flow velocity it again becomes negative $g < 0$. The shape of the flutter

mode is characterized by antiphase vibration of right and left control surfaces: the left control surface has bending-rotation vibrations and the right control surface has only bending vibrations. Vibrations of the left control surface are with greater amplitudes than of the right control surface.

In Table 7 comparison of experimental and calculated critical speed and critical frequencies of flutter for Configuration 1 is given. Critical speed is given in relative values and rated by V_0 = const.

ρ, kg/m^3	Mach num.	EMM		KC-M		Nastran		RIF	
		V, m/s	*f*, Hz	*V*, m/s	*f*, Hz	*V*, m/s	*f*, Hz	*V*, m/s	*f*, Hz
1.225	0.4	233	14	240	17	249	17	226	17
1	0.4	258	14	266	17	276	17	251	17
0.8	0.4	287	14	298	17	309	17	281	16
0.6	0.4	330	14	345	16	358	17	327	16
1.225	1.1	327	15	278	16	293	16	---	---
1	1.1	367	15	308	16	325	16	---	---
0.8	1.1	406	15	348	16	364	16	---	---
0.6	1.1	473	15	385	16	425	16	---	---

Table 7: Experimental and calculated critical speed and critical frequencies comparison for Configuration 1.

Calculations for program RIF haven't been done in supersonic region. In subsonic region the results of flutter calculations for three programs are similar. In supersonic region for KC-M, Nastran and EMM there is a difference between the critical speed of flutter and the critical frequency.

The difference between the values of the experimental and the calculated flutter frequency is that in Configuration 1 eigen modes distinguish from the experimental ones.

In Table 8 comparison of experimental and calculated critical speed and critical frequencies of flutter for Configuration 2 is given. As for Configuration 1 critical speed is given in relative values and rated by V_0 = const.

ρ, kg/m^3	Mach num.	EMM		KC-M		Nastran		RIF	
		V, m/s	*f*, Hz	*V*, m/s	*f*, Hz	*V*, m/s	*f*, Hz	*V*, m/s	*f*, Hz
1.225	0.4	233	14	224	14	221	14	242	13
1	0.4	258	14	248	14	246	14	268	13
0.8	0.4	282	14	279	14	275	14	301	13
0.6	0.4	330	14	323	14	318	14	348	13
1.225	1.1	327	15	281	14	269	14	---	---
1	1.1	367	15	300	14	298	14	---	---
0.8	1.1	406	15	342	14	335	14	---	---
0.6	1.1	473	15	392	14	387	14	---	---

Table 8: Experimental and calculated critical speed and critical frequencies comparison for Configuration 2.

In subsonic (KC-M, Nastran, RIF) region values of the critical speed and the frequency of flutter are quite similar experimental values and in supersonic (KC-M, Nastran) there is a difference. For Configuration 2 general change in the critical speed of flutter with a change in the air flow density and Mach number is the same for different mathematical models and different programs, and also in the experiment.

For both configurations there is a difference in numerical value of the flutter boundary received from calculations in comparison with value of the flutter boundary obtained in the EMM experiment. The cumulative causes are the imperfections of the elastic-mass schemes of mathematical models that don't take into account the presence of a "side" resonance (inaccessible mass of the actuator in the body) and the nonlinear characteristics of the structure, as well as the difference in aerodynamic theories.

3 CONCLUSION

The data of flutter calculations of an elastic model with different stiffnesses of control surfaces are presented. Based on the results of GVT, dynamic elastic-mass mathematical models were corrected.

Flutter calculations conducted with KC-M, Nastran and RIF programs gave close values of critical speed and critical frequency of flutter.

The experiment on the model with artificial flow with EMM allowed to obtain similar dependencies of the critical speed of flutter on air flow regimes as air density and Mach numbers to that in the calculations.

The difference between the calculation results and the experiment data is due to the imperfection of the calculation schemes - without taking into account inaccessible elastically suspended masses, nonlinearity of structural characteristics and differences in aerodynamic theories.

4 ACKNOWLEDGEMENT

The first author thanks the Dmitriy Kazantsev, Aleksei Orlov, Sergei Paryshev for their help in this work.

5 REFERENCES

[1] Prodera modal analysis systems and software. Technical articles. http://www.prodera.com/uk/prodera_articles.html.

[2] P. Karkle, M. Pronin, V. Smyslov. Wing's flutter bench investigations with the modeling of aerodynamic forces. 15th International Forum on Aeroelasticity and Structural Dynamics, 27 - 30 June 2011, Paris, France, 2011

[3] A.G. Narizhnyi, V.I. Smyslov. About influence of asymmetry stiffness characteristics on vibration of aircraft constructions. «Vibrations of elastic structures with liquid. Collection of scientific reports of the 5th symposium», 1984.

[4] Program system KC-M user guide (ver 2011.1), TsAGI.

[5] MSC.Nastran 2012. Quick Reference Guide. MSC.Flight Loads and Dynamics User's Guide Version 2008 (r1)

COPYRIGHT STATEMENT